International Journal of Bifurcation and Chaos, Vol. 20, No. 2 (2010) 287–295

DOI: 10.1142/S0218127410025739

SPONTANEOUS SYMMETRY BREAKING AND FIRST-ORDER PHASE TRANSITIONS OF ADSORBED FLUIDS

SALVADOR A. SARTARELLI
Instituto de Desarrollo Humano,
Universidad Nacional de General Sarmiento,
Gutierrez 1150, RA–1663 San Miguel, Argentina

LESZEK SZYBISZ* and IGNACIO URRUTIA
Laboratorio TANDAR, Departamento de Física,
Comisión Nacional de Energía Atómica, Av. del Libertador 8250,
RA–1429 Buenos Aires, Argentina

Departamento de Física, Facultad de Ciencias Exactas y Naturales,
Universidad de Buenos Aires, Ciudad Universitaria,
RA–1428 Buenos Aires, Argentina

Consejo Nacional de Investigaciones Científicas y Técnicas,
Av. Rivadavia 1917, RA–1033 Buenos Aires, Argentina
**szybisz@tandar.cnea.gov.ar*

Received December 1, 2008; Revised March 31, 2009

A density functional formalism is applied to investigate the wetting behavior of Ne confined in slits composed of two parallel solid identical alkaline walls with increasing attractive strength leading to a variety of wetting situations. The study is performed over the complete range of temperature spanned from the triple point T_t up to the critical one T_c of Ne. Attention is paid to the slit's width. It was found that in the case of weaker substrates for temperatures below a certain critical T_{sb} the density profiles corresponding to the lowest free energy are asymmetric, i.e. exhibit a spontaneous breaking of symmetry. For $T > T_{sb}$ the phenomenon of symmetry breaking disappears leading to a first-order phase transition.

Keywords: Adsorption of fluids; growth of films; interfaces and wetting phenomena.

1. Introduction

The adsorption of fluids in confined geometries has been extensively studied for several decades. In these cases the fluid is attracted by solid walls and exhibits liquid (l) and vapor (v) phases. The competing fluid–fluid (f–f) and solid–fluid (s–f) attractions determine the density profile $\rho(\mathbf{r})$ of the adsorbed particles. In pioneering works van Leeuwen and collaborators [Sikkenk *et al.*, 1987; Nijmeijer *et al.*, 1990] applied molecular-dynamics simulations for investigating the behavior of a fluid in slits composed of two parallel identical planar walls. Starting from a situation where the well depth of the s–f attraction, D, is weaker than that of the f–f one, ε_{ff}, and by increasing the relative strength $\varepsilon_r = D/\varepsilon_{ff}$ they obtained drying, partial wetting

*Author for correspondence

and complete wetting. Drying is characterized by the fact that for a given T the peak of the fluid density distribution located close to the substrate is lower than the corresponding liquid saturation density. In the case of partial wetting, the density profiles of the fluid are asymmetric, being liquid on one wall and vapor on the other. For complete wetting the profiles are symmetric exhibiting liquid phase on both walls. The behavior depends on the balance of surface tensions corresponding to s–l, l–l, and l–v interfaces. An interesting task is to search whether there are in nature systems which may show such a pattern.

Looking for the possibility of finding asymmetric density profiles in real systems, Berim and Ruckenstein [2007] analyzed the case of Ar adsorbed in planar slits of CO_2. They assumed that atoms of Ar interact via a spherically symmetric (12–6) Lennard–Jones (LJ) potential $V_{\rm LJ}(r) = 4\varepsilon_{ff}[(\sigma_{ff}/r)^{12} - (\sigma_{ff}/r)^6]$ characterized by the well depth ε_{ff} and size σ_{ff} and the s–f interaction is given by a widely used (9–3) model potential $U_{sf}(z) = 4C_3^3/27D^2z^9 - C_3/z^3$ of depth D and van der Waals tail C_3 [Ebner & Saam, 1977], where z stands for the distance perpendicular to the substrate plane. The behavior for a slit of reduced width $L^* = L/\sigma_{ff} = 15$ was examined. These authors claimed that a spontaneous symmetry breaking occurs for temperatures below the critical value $T_{sb} = 106\,\mathrm{K}$. In a recent paper [Szybisz & Sartarelli, 2008] we revisited the investigation of [Berim & Ruckenstein, 2007] finding that, indeed, their conclusion was based on calculations performed with a s–f potential which includes a hard-wall repulsion located in such a way that the depth of the s–f potential, D, was diminished. In fact, when the original [Ebner & Saam, 1977] potential is used, the spontaneous symmetry breaking disappears, i.e. the density profiles become symmetric at all temperatures T in the range spanned from the triple point T_t up to the critical one T_c of Ne.

In searching for systems which could undergo spontaneous symmetry breaking, one may verify that a favorable ratio $\varepsilon_r = D/\varepsilon_{ff}$ is exhibited by inert gases adsorbed on surfaces of alkali metals (see e.g. Table I in [Curtarolo *et al.*, 2000]). The aim of present work is just to report the results of a study of the adsorption of Ne in slits of alkali walls. The calculations were carried out using the density functional (DF) formalism of [Kierlik & Rosinberg, 1990] (henceforth KR). The analysis was performed at temperatures in the range $T_t \le T \le T_c$ for slits of different widths $L^* = 30$, and 40. Let us note that the calculations of [Sikkenk *et al.*, 1987] were done for $L^* = 29.1$, while $L^* = 40$ is the size of the largest slit examined by [Maciolek *et al.*, 2003] in a more recent work on the effects of weak surface fields on the density profiles and adsorption of a confined fluid near bulk criticality. The width of these slits guarantee that the interaction between fluid atoms located close to opposite walls is negligible.

The paper is organized as follows. In Sec. 2, the theoretical framework is outlined. The results are given in Sec. 3. Finally, Sec. 4 is devoted to conclusions.

2. Theoretical Background

In this section, we shall describe the fundamentals of a DF, the pair potential accounting for the f–f interaction, the adsorption potential and the Euler–Lagrange (E–L) equation which determines the density profile.

2.1. *Density functional*

Let us now outline the main features of a mean field DF theory. In such a formalism, the Helmholtz free energy $F_{DF}[\rho(\mathbf{r})]$ of an inhomogeneous fluid embedded in an external potential $U_{sf}(\mathbf{r})$ is expressed as a functional of the local density $\rho(\mathbf{r})$ (see e.g. [Ravikovitch *et al.*, 2001]):

$$F_{DF}[\rho(\mathbf{r})] = \nu_{\rm id}\, k_B\, T \int d\mathbf{r}\, \rho(\mathbf{r})\, \{\ln[\Lambda^3\rho(\mathbf{r})] - 1\} + \int d\mathbf{r}\, \rho(\mathbf{r})\, f_{\rm HS}[\overline{\rho}(\mathbf{r}); d_{\rm HS}] + \frac{1}{2}\iint d\mathbf{r}\, d\mathbf{r}'\, \rho(\mathbf{r})\, \rho(\mathbf{r}'')\, \Phi_{\rm attr}(|\mathbf{r} - \mathbf{r}'| + \int d\mathbf{r}\, \rho(\mathbf{r})\, U_{sf}(\mathbf{r}). \quad (1)$$

The first term is the ideal gas free energy, $F_{\rm id}(\mathbf{r})$, where k_B is the Boltzmann constant and $\Lambda = \sqrt{2\,\pi\,\hbar^2/m\,k_B\,T}$ the thermal de Broglie wavelength of the molecule of mass m. Quantity $\nu_{\rm id}$ is a parameter introduced in Eq. (2) of [Ancilotto *et al.*, 2001], in the standard theory it equals unity. The second term accounts for the repulsive f–f interaction usually approximated by a hard-sphere (HS) functional, $F_{\rm HS}(\mathbf{r})$, with a certain choice for the HS diameter $d_{\rm HS}$. The third term is the attractive f–f interactions treated in a

mean field approximation (MFA). Finally, the last integral represents the effect of the external potential exerted on the fluid.

In the present work the inhomogeneous HS contribution is described by the expression for $f_{\rm HS}[\overline{\rho}(\mathbf{r}); d_{\rm HS}]$ provided by the KR nonlocal DF (NLDF) formalism [Kierlik & Rosinberg, 1990] where $\overline{\rho}(\mathbf{r})$ is a properly averaged density. In the limit of uniform fluid, the KR form yields the compressibility equation of state of [Percus & Yevick, 1958] as given by Eq. (6.44) in [Baker & Henderson, 1976]. The attractive part of the f–f interaction was described by an effective pair interaction which is a variant of the raw LJ potential proposed quite recently [Sartarelli *et al.*, 2009]. We assume that fluid atoms and walls interact via the *ab initio* potential derived by [Chizmeshya *et al.*, 1998] (henceforth CCZ) with parameters listed in Table 1 therein.

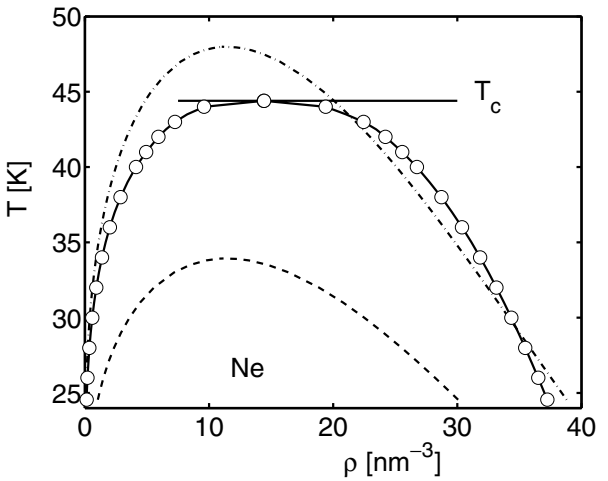

Fig. 1. Phase diagram of bulk Ne. The circles denote the experimental coexistence curve taken from [Rabinovich *et al.*, 1988]. The dashed line corresponds to the bare LJ potential. The dot-dashed line is the standard WCA result. The solid line is the three-parameter fit (see text).

2.2. *Effective pair potential*

The effective pair potential used in the present work is based on the separation introduced by Weeks, Chandler and Andersen (WCA) in their perturbation theory of fluids [Weeks *et al.*, 1970] (see Fig. 1 therein)

$$\Phi_{\rm attr}^{\rm WCA}(r) = \begin{cases} -\tilde{\varepsilon}_{ff}, & r \le r_m \\ 4\tilde{\varepsilon}_{ff}\left[\left(\dfrac{\tilde{\sigma}_{ff}}{r}\right)^{12} - \left(\dfrac{\tilde{\sigma}_{ff}}{r}\right)^{6}\right], & r > r_m, \end{cases} \tag{2}$$

where $r_m = 2^{1/6}\tilde{\sigma}_{ff}$ is the position of the LJ minimum. No cut off for the pair potential was introduced. This effective interaction preserves the long range behavior $-r^{-6}$ of the original bare LJ potential, which is important when studying adsorption properties. In the present WCA (WCA-PW), we consider $\tilde{\varepsilon}_{ff}$ and $\tilde{\sigma}_{ff}$ as free parameters. Hence, the complete formalism has three adjustable parameters (namely, ν_{id}, $\tilde{\varepsilon}_{ff}$, and $\tilde{\sigma}_{ff}$), which were determined by imposing on the bulk l–v coexistence curve for Ne to be reproduced. This curve may be determined by using expressions for P and μ provided by Eq. (1) in the case of a uniform fluid of density ρ

$$\begin{aligned} P(T) &= P_{\rm HS}(T) + \frac{b}{2}\rho^2 \quad \text{and} \\ \mu(T) &= \mu_{\rm HS}(T) + b\,\rho, \end{aligned} \tag{3}$$

with $b = \int d\mathbf{r}\Phi_{\rm attr}(r)$. In the present work, $P_{\rm HS}$ and $\mu_{\rm HS}$ were evaluated by using the compressibility expressions in [Percus & Yevick, 1958] as given in [Barker & Henderson, 1976] which are compatible with the KR formulation. When $\Phi_{\rm attr}(r)$ is the attractive part of the bare LJ potential, one gets $b_{\rm LJ} = -(32\pi/9)\varepsilon_{ff}\sigma_{ff}^3$. At coexistence, the pressure as well as the chemical potential of the v and l phases should be equal

$$P(\rho_v) = P(\rho_l) \quad \text{and} \quad \mu(\rho_v) = \mu(\rho_l). \tag{4}$$

By imposing these conditions on Ne, the bare LJ with the standard parameters $\varepsilon_{ff}/k_B = 33.9$ K and $\sigma_{ff} = 0.278$ nm (see e.g. [Ancilotto & Toigo, 1999]) lead to the coexistence curve displayed in Fig. 1. These theoretical results are much lower than the experimental data taken from Table III of [Rabinovich *et al.*, 1988]. In order to study quantitatively the adsorption of fluids within a DF approach, one must require that the experimental bulk equation of state (EOS) and l–v surface tension γ_{lv} be reproduced as well as possible in the whole range of temperatures $T_t \le T \le T_c$.

In practice, we set $d_{\rm HS} = \tilde{\sigma}_{ff}$ and required that condition (4) be satisfied for the quantities ρ_v, ρ_l and $P(\rho_v) = P(\rho_l) = P_0$ listed in Table III of [Rabinovich *et al.*, 1988]. For $\Phi_{\rm attr}^{\rm WCA}(r)$ one gets $b_{\rm PW} = -(32\sqrt{2}\,\pi/9)\tilde{\varepsilon}_{ff}\tilde{\sigma}_{ff}^3$. This procedure yields the values listed in Table 1. Of course, as indicated in Fig. 1, the coexistence curve is reproduced and, in addition, as shown in [Sartarelli *et al.*, 2009] this approach yields a surface tension γ_{lv} in agreement with experimental data as well as with

Table 1. Values of $\nu_{\rm id}$, $\tilde{\sigma}_{ff}/\sigma_{ff}$ and $\tilde{\varepsilon}_{ff}/\varepsilon_{ff}$ obtained from the fit of the experimental coexistence curve at bulk saturation vapor pressure of Ne (see explanation in the text).

T (K)	P_0^* $(P_0(\sigma_{ff}^3/\varepsilon_{ff}))$	ρ_v^* $(\rho_v\sigma_{ff}^3)$	ρ_l^* $(\rho_l\sigma_{ff}^3)$	ν_{id}	$\tilde{\varepsilon}_{ff}/\varepsilon_{ff}$	$\tilde{\sigma}_{ff}/\sigma_{ff}$
24.55	0.00199	0.00283	0.80013	0.99420	0.93398	1.00079
25.	0.00234	0.00328	0.79537	0.99309	0.93443	0.99923
26.	0.00330	0.00449	0.78447	0.99184	0.93609	0.99595
27.	0.00452	0.00599	0.77339	0.99002	0.93723	0.99257
28.	0.00606	0.00784	0.76199	0.98815	0.93818	0.98919
29.	0.00796	0.01009	0.75013	0.98577	0.93868	0.98578
30.	0.01027	0.01280	0.73796	0.98306	0.93887	0.98229
31.	0.01304	0.01601	0.72535	0.97985	0.93867	0.97871
32.	0.01631	0.01982	0.71222	0.97619	0.93808	0.97504
33.	0.02013	0.02431	0.69856	0.97208	0.93712	0.97122
34.	0.02457	0.02960	0.68417	0.96680	0.93538	0.96720
35.	0.02966	0.03577	0.66896	0.96156	0.93358	0.96312
36.	0.03547	0.04305	0.65282	0.95505	0.93097	0.95875
37.	0.04207	0.05153	0.63535	0.94949	0.92877	0.95450
38.	0.04948	0.06176	0.61700	0.94021	0.92451	0.94926
39.	0.05784	0.07381	0.59634	0.93271	0.92099	0.94437
40.	0.06711	0.08829	0.57443	0.92379	0.91699	0.93872
41.	0.07749	0.10586	0.54933	0.91603	0.91342	0.93316
42.	0.08901	0.12725	0.52034	0.91080	0.91117	0.92797
42.5	0.09513	0.14011	0.50418	0.90689	0.90957	0.92496
43.	0.10172	0.15583	0.48237	0.90327	0.90707	0.92293
43.5	0.10848	0.17705	0.45161	0.89458	0.90102	0.92125
44.	0.11577	0.20633	0.41682	0.88281	0.89402	0.91720
44.40	0.12178	0.30999	0.30999	0.83813	0.86899	0.90600

predictions given by the fluctuation theory of critical phenomena. The results for $\tilde{\sigma}_{ff}/\sigma_{ff}$ at temperatures $39 \leq T \leq 44\,\mathrm{K}$ can be compared with those listed in Table II of [Ancilotto & Toigo, 1999], the agreement between both sets of values is good. It is important to note that the WCA form when computed with the bare values ε_{ff} and σ_{ff} overestimates T_c as shown in Fig. 1 (see also Fig. 2 in [Ravikovitch *et al.*, 2001]).

2.3. *Euler–Lagrange equation for a slit geometry*

The equilibrium density profile $\rho(\mathbf{r})$ of the fluid adsorbed in a closed slit is determined by a minimization of the free energy with respect to density variations with the constraint of a fixed number of particles N

$$\frac{\delta}{\delta\rho(\mathbf{r})}\left[F_{DF}[\rho(\mathbf{r})] - \mu\int d\mathbf{r}\,\rho(\mathbf{r})\right] = 0. \qquad (5)$$

Here, i.e. for an ensemble with fixed V, T and N, the Lagrange multiplier μ is an unknown quantity which should be determined from the constraint. Hence, it is not necessarily equal to $\mu_{\rm coex}$ of an open slit in equilibrium with a reservoir at temperature T (see e.g. [Ancilotto & Toigo, 1999]).

We assume that in a planar symmetry where the walls exhibit an infinite extent in the x and y directions, the profile depends only on the coordinate z perpendicular to the substrate. For this geometry, the variation of Eq. (5) yields the following E–L equation

$$\frac{\delta[F_{\rm id}+F_{\rm HS}]}{\delta\rho(z)} + \int_0^L dz'\,\rho(z')\,\overline{\Phi}_{\rm attr}(\mid z-z'\mid) + U_{sf}(z) = \mu, \qquad (6)$$

where

$$\frac{\delta F_{\rm id}}{\delta\rho(z)} = \nu_{\rm id}k_B\,T\,\ln[\Lambda^3\,\rho(z)], \qquad (7)$$

and

$$\frac{\delta F_{\rm HS}}{\delta\rho(z)} = f_{\rm HS}[\overline{\rho}(z);d_{\rm HS}] + \int_0^L dz'\,\rho(z')\,\frac{\delta f_{\rm HS}[\overline{\rho}(z');d_{\rm HS}]}{\delta\overline{\rho}(z')}\,\frac{\delta\overline{\rho}(z')}{\delta\rho(z)}. \qquad (8)$$

So, the final E–L equation for a slit of width L may be cast into the form

$$\nu_{\rm id}\, k_B\, T\, \ln\left[\Lambda^3\, \rho(z)\right] + Q(z) = \mu. \tag{9}$$

where

$$\begin{aligned} Q(z) = {} & f_{\rm HS}[\overline{\rho}(z); d_{\rm HS}] \\ & + \int_0^L dz'\, \rho(z')\, \frac{\delta f_{\rm HS}[\overline{\rho}(z'); d_{\rm HS}]}{\delta \overline{\rho}(z')}\, \frac{\delta \overline{\rho}(z')}{\delta \rho(z)} \\ & + \int_0^L dz'\, \rho(z')\, \overline{\Phi}_{\rm attr}(|z - z'|) + U_{sf}(z). \end{aligned} \tag{10}$$

The number of particles N per unit area of one wall A in a slit (coverage) is

$$N_s = \frac{N}{A} = \int_0^L \rho(z)\, dz. \tag{11}$$

In order to get solutions for $\rho(z)$, it is useful to rewrite Eq. (9) as

$$\rho(z) = \rho_0\, \exp\left(-\frac{Q(z)}{\nu_{\rm id}\, k_B\, T}\right), \tag{12}$$

with

$$\rho_0 = \frac{1}{\Lambda^3}\, \exp\left(\frac{\mu}{\nu_{\rm id}\, k_B\, T}\right). \tag{13}$$

The relation between μ and N_s is obtained by substituting Eq. (12) into the constraint given by Eq. (11)

$$\mu = -\nu_{\rm id}\, k_B\, T\, \ln\left[\frac{1}{N_s\, \Lambda^3} \int_0^L dz\, \exp\left(-\frac{Q(z)}{\nu_{\rm id}\, k_B\, T}\right)\right]. \tag{14}$$

3. Analysis and Results

The E–L equation was solved for fixed values of the number of particles per area of one wall, N_s, which for a slit of width L yields an average fluid density $\rho_{\rm av} = N_s/L$. Figure 2 shows the adsorption potentials for Ne on Rb, Na, Li, and Mg taken from [Chizmeshya *et al.*, 1998]. The potentials for Ne/Cs and Ne/K are very similar to that for Ne/Rb, therefore are not included in the plot. When solving this kind of systems, it is usual to define dimensionless variables $z^* = z/\tilde{\sigma}_{ff}$ for the distance and $\rho^* = \rho\, \tilde{\sigma}_{ff}^3$ for the densities. In these units the width becomes $L^* = L/\tilde{\sigma}_{ff}$ and the average density $\rho^*_{\rm av} = N_s\, \tilde{\sigma}_{ff}^3/L = N_s^*/L^*$. Let us first present the types of solutions with lowest free energy per one wall surface, $f_{DF} = F_{DF}/A$, which may be obtained for this

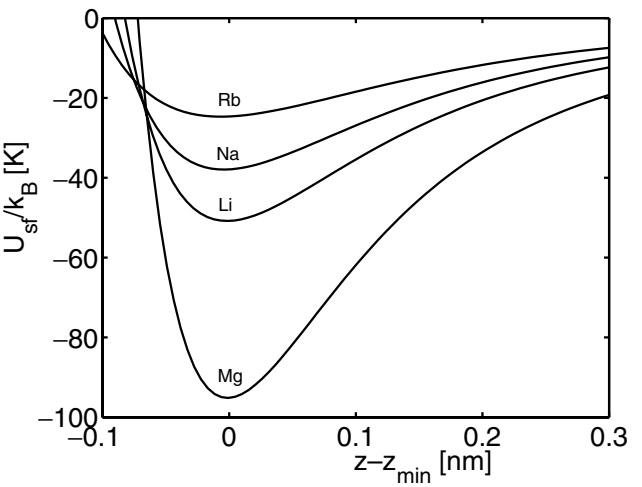

Fig. 2. Comparison of CCZ adsorption potentials for Ne on alkali substrates, the curves are centered at the corresponding minimum.

kind of systems and, subsequently, to describe the main results of our work. Figure 3 shows three possible shapes of density profiles yielded in the case of Ne confined in a slit of Li for $L^* = 30$ at $T = 26$ K. These results were obtained by increasing coverage and are the common pattern for alkali metals close to T_t. A symmetric accumulation of Ne atoms at the walls is obtained for small average density (dash-dotted curve), for intermediate coverage the solution is asymmetrical (solid curve), while for even larger coverages a symmetric capillary condensation

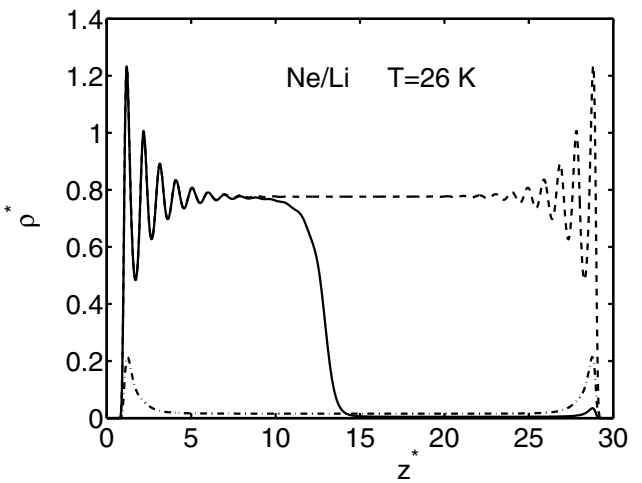

Fig. 3. Typical density profiles of Ne confined in a slit of Li with $L^* = 30$ at $T = 26$ K as a function of the distance from the left wall. A symmetric thin film (dash-dotted curve) is shown for $\rho^*_{\rm av} = 0.0256$, an asymmetric film (solid curve) is plotted for $\rho^*_{\rm av} = 0.3066$, and the capillary condensation (dashed curve) corresponds to $\rho^*_{\rm av} = 0.7286$.

is obtained (dashed curve). In the case of asymmetric profiles, the situation is termed as partial (or one wall) wetting.

The evolution of solutions for increasingly attractive walls is shown in Fig. 4. This plot shows density profiles in slits of identical walls of Rb, Li, and Mg of width $L^* = 30$. In all cases the results correspond to $\rho^*_{\rm av} = 0.1533, 0.2300$, and 0.3066 at $T = 26$ K. One may observe that for Rb and Li the profiles are asymmetrical, while for Mg, which is the most attractive substrate of this series, $\rho^*(z^*)$ becomes symmetrical. The profiles shown in Figs. 4(a) and 4(b) exhibit a fluid sector on the left wall with density oscillating about the bulk liquid density at coexistence ρ^*_l and a small peak of vapor on the right wall. A comparison of the three drawings in Fig. 4 indicates that the amplitude of the layering increases for increasing wall attraction. Furthermore, it is important to mention that in the cases of Ne/Rb and Ne/Li profiles displayed in Figs. 4(a) and 4(b) there are also solutions with the same free energy but with inverse asymmetry, i.e. with the liquid phase close to the right wall.

The results displayed in Fig. 4 may be understood on the basis of the discussion reported in [Sikkenk *et al.*, 1987]. In general, this kind of systems can support solid–liquid (sl), solid–vapor (sv), and liquid–vapor (lv) interfaces. The structure of the profiles depends on the balance of the involved surface tensions γ_{sl}, γ_{lv} and γ_{sv} which are related by the Young's law (see e.g. Eq. (1.1) in [Nijmeijer *et al.*, 1990])

$$\gamma_{sv} = \gamma_{sl} + \gamma_{lv} \cos\theta, \tag{15}$$

where θ is the contact angle. The latter quantity is defined as the angle between the wall and the interface between the liquid and the vapor and it depends on the ratio of strengths, $\varepsilon_r = D/\varepsilon_{ff}$. For increasing ε_r three cases may be observed:

(i) at low ε_r, *symmetric* profiles consisting of two sv interfaces and two lv interfaces are obtained, this situation corresponds to a complete wall drying as can be seen in Fig. 1 in [Nijmeijer *et al.*, 1990];

(ii) at intermediate ε_r, *asymmetric* profiles consisting of a sl, a lv and a sv interface are obtained, here the wall attraction is sufficiently strong to produce a partial wetting, i.e. to support a rather thick film on one wall while a sv interface is present near the other wall, this feature is exhibited by the Ne/Li system in Fig. 4(b);

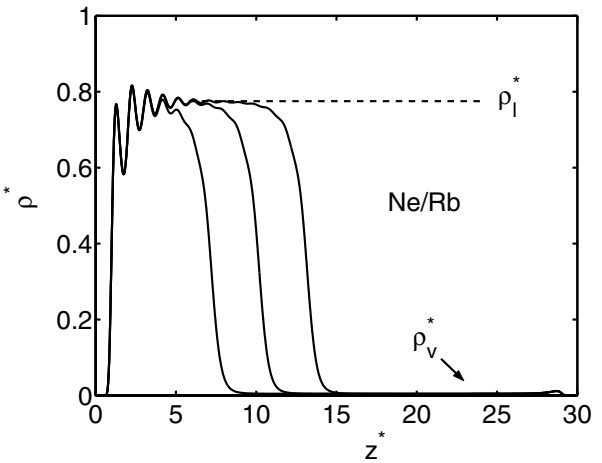

(a)

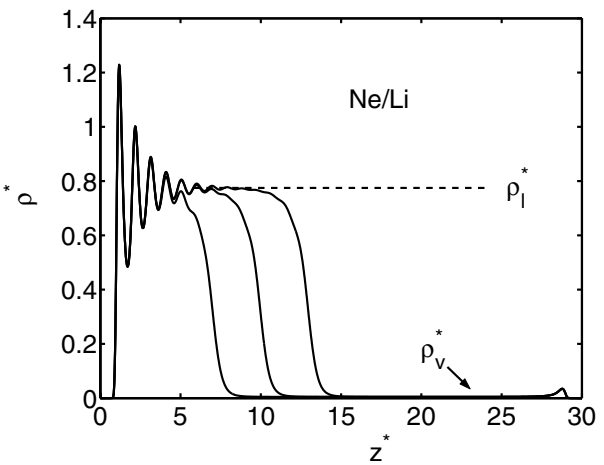

(b)

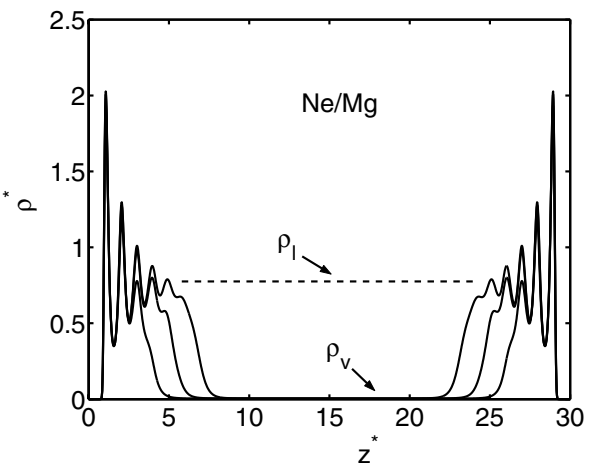

(c)

Fig. 4. Density profiles of the indicated systems confined in a slit of $L^* = 30$ at $T = 26$ K. The displayed data correspond to average densities $\rho^*_{\rm av} = 0.1533, 0.2300$ and 0.3066. The dashed lines are the densities of bulk l–v coexistence at $T = 26$ K.

(iii) for the largest ε_r, *symmetric* profiles consisting of two *sl* interfaces and two *lv* interfaces are obtained, now the strength is enough to wet both walls as can be seen in the case of the Ne/Mg system in Fig. 4(c).

The transition from (i) to (ii) takes place at the drying point $\theta = \pi$, whereas the transition from (ii) to (iii) takes place at the wetting point $\theta = 0$.

The asymmetric profiles change with temperature. Figure 5 shows the dependence on temperature of an asymmetric profile in the case of the system Ne/Li for a slit of $L^* = 30$. One may realize that starting from an asymmetric profile at $T = 26$, when one increases the temperatures, there is a transmission of particles towards the vapor film and eventually the system undergoes a first-order phase transition to a symmetric situation corresponding to a complete (or two walls) wetting. This change of phase occurs at a critical temperature T_{sb}, which is lower for more attractive walls. Due to this property the density profile in a slit of Mg shown in Fig. 4(c) is already symmetrical at T_t.

The asymmetric profiles plotted in Figs. 3–5 exhibit larger amount of fluid on the left wall. However, it should be noticed that, indeed, there are two equivalent asymmetric solutions (i.e. with the same free energy). One of them $\rho_1^*(z^*)$ has more fluid on one wall, while the other $\rho_2^*(z^*)$ has more fluid on the opposite wall satisfying the relation $\rho_2^*(z^*) = \rho_1^*(L^* - z^*)$. An experimental setup may indifferently produce any one of these solutions.

The asymmetry of density profiles may be measured by the quantity

$$\Delta_N = \frac{1}{N_s} \int_0^{L/2} dz\, [\rho(z) - \rho(L - z)]. \qquad (16)$$

According to this definition, if the profile is completely asymmetrical about the middle of the slit, i.e. for: (i) $\rho(z < L/2) \neq 0$ and $\rho(z \geq L/2) = 0$; or (ii) $\rho(z < L/2) = 0$ and $\rho(z \geq L/2) \neq 0$ this quantity becomes $+1$ or -1, respectively, while for symmetric solutions it vanishes.

The evolution of Δ_N as a function of the average density for the Ne/Rb system is shown in Fig. 6. Data corresponding to two widths $L^* = 30$ and 40 and two temperatures $T = 25$ and 38 are displayed. In all the cases, starting from very low coverages the lowest f_{DF} corresponds to symmetric profiles, i.e. $\Delta_N = 0$, then at a certain value ρ_{sb1}^* the symmetric solution becomes an excited state and the lowest f_{DF} corresponds to asymmetric species. At this point the plot shows a bifurcation since there are two shapes one with positive Δ_N and another with negative Δ_N both exhibiting exactly the same f_{DF}. This situation continues until ρ_{sb2}^* where the asymmetric solutions disappear, the loop of Δ_N closes, and a symmetric capillary condensation (like the dashed profile of Fig. 3) becomes the lowest lying state. Since results for $L^* = 30$ and 40 are quite similar, one could conjecture that these slits have already reached the appropriate size for this kind of study. The loop corresponding to

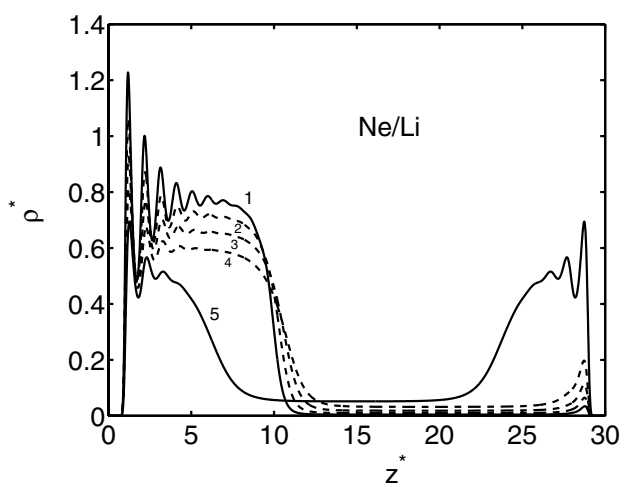

Fig. 5. Density profiles of Ne confined in a Li slit of width $L^* = 30$ as a function of the reduced distance $z^* = z/\tilde{\sigma}_{ff}$. Data numbered from 1 to 5 correspond to $T = 26, 29, 32, 35$, and 38 K, respectively. One may observe the transition from asymmetric to symmetric profiles.

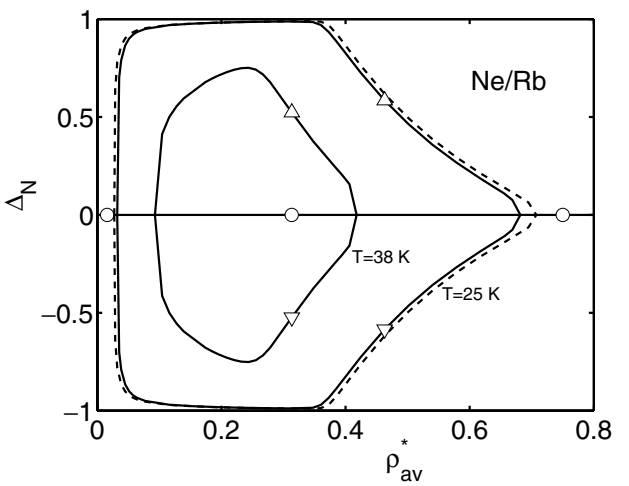

Fig. 6. Asymmetry parameter for the system Ne/Rb as a function of average density. The solid curves correspond to a slit of $L^* = 30$ at the two temperatures indicated. The dashed curve shows results for $L^* = 40$. The asymmetric solutions occur for different ranges $\rho_{sb1}^* < \rho_{\rm av}^* < \rho_{sb2}^*$.

$T = 38$ K is smaller than that for $T = 25$ K. The range $\rho^*_{sb1} < \rho^*_{\rm av} < \rho^*_{sb2}$, where the asymmetric solutions occur diminishes for increasing temperature and becomes zero at $T = T_{sb}$.

Since the results for the slits of $L^* = 30$ and 40 are very similar in general, not only for the asymmetry shown in Fig. 6, also for the present work we restrict ourselves to report data for the smaller system.

Let us now refer to the chemical potential. In Fig. 7, we plotted μ as a function of average density for the system Ne/Rb for $L^* = 30$ and $T = 25$ K. The asymmetric solutions occur in the range $\rho^*_{sb1} < \rho^*_{\rm av} < \rho^*_{sb2}$, at the central part of this interval the values present a plateau which agrees in the scale of the drawing with $\mu_{\rm coex}$ at $T = 25$ K. At the ends of the density interval μ exhibits deviations toward the values corresponding to symmetric solutions. Furthermore, one can now understand the nature of the small vapor peaks present in the profiles displayed in Figs. 4(b) and 4(c), they correspond to thin films in coexistence with thick ones as indicated in Fig. 7. It is interesting to note that in the cases of both sorts of symmetric solutions close to the extremes (maximum and minimum) of μ there are bifurcations between stable and unstable profiles.

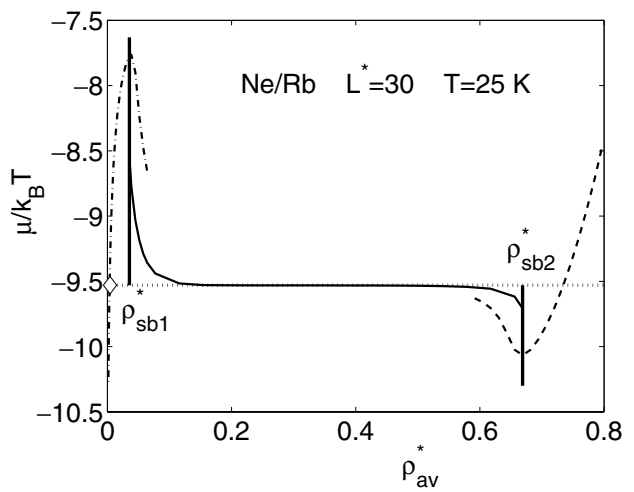

Fig. 7. Chemical potential of the indicated system as a function of the average density. The solid curve shows results for the asymmetric solution, the existence of this sort of profiles is restricted to the interval determined by the solid vertical lines. The dashed and dash-dotted curves correspond to symmetric thin films and to the capillary condensation, respectively. The dotted line stands for $\mu_{\rm coex}$. The diamond indicates the thin film in coexistence with asymmetric profiles of the plateau.

4. Conclusions

The confinement of Ne in slits composed of two identical walls of alkali surfaces was studied within the DF framework by utilizing realistic interactions. Two rather wide slits of $L^* = 30$ and 40 were analyzed and both series of results do not show important differences. It was found that for alkali–metal substrates below a certain temperatures T_{sb}, there is a range of average densities $\rho^*_{sb1} < \rho^* < \rho^*_{sb2}$ for which the state with lowest free energy exhibits asymmetric density profiles. This behavior can be understood in terms of the balance of involved surface tensions. For the alkali–earth substrate, which is the most attractive of the examined slits, there is complete wetting close to T_t. We are planning to do similar calculations for the other inert gases.

To the best of our knowledge these are the first realistic calculations showing that in the case of a slit geometry, there are systems which would exhibit asymmetric profiles. We suggest to check experimentally our theoretical findings.

Acknowledgments

This work was supported in part by the Ministry of Culture and Education of Argentina through Grants CONICET PIP No. 5138/05, ANPCyT PICT Nos. 492 and 31980, and UBACYT No. X298.

References

Ancilotto, F. & Toigo, F. [1999] "Prewetting transitions of Ar and Ne on alkali-metal surfaces," *Phys. Rev. B* **60**, 9019–9025.

Ancilotto, F., Curtarolo, S., Toigo, F. & Cole, M. W. [2001] *Phys. Rev. Lett.* **87**, 206103-1–206103-4.

Barker, J. A. & Henderson, D. [1976] "What is "liquid"? Understanding the states of matter," *Rev. Mod. Phys.* **48**, 587–671.

Berim, G. O. & Ruckenstein, E. [2007] "Symmetry breaking of the fluid density profiles in closed nanoslits," *J. Chem. Phys.* **126**, 124503-1–124503-8.

Chizmeshya, A., Cole, M. W. & Zaremba, E. [1998] "Weak biding potentials and wetting transitions," *J. Low Temp. Phys.* **110**, 677–682.

Curtarolo, S., Stan, G., Bojan, M. J., Cole, M. W. & Steele, W. A. [2000] "Threshold criterion for wetting at the triple point," *Phys. Rev. E* **61**, 1670–1675.

Ebner, C. & Saam, W. F. [1977] "New phase-transition phenomenon in thin argon films," *Phys. Rev. Lett.* **38**, 1486–1489.

Kierlik, E. & Rosinberg, M. L. [1990] "Free-energy density functional for the inhomogeneous hard-sphere

fluid: Application to interfacial adsorption," *Phys. Rev. A* **42**, 3382–3387.

Maciolek, A., Evans, R. & Wilding, N. B. [2003] "Effects of weak surface fields on the density profiles and adsorption of a confined fluid near bulk criticality," *J. Chem. Phys.* **118**, 8663–8675.

Nijmeijer, M. J. P., Bruin, C., Bakker, A. F. & van Leeuwen, J. M. J. [1990] "Wetting and drying of an inert wall by a fluid in a molecular-dynamics simulation," *Phys. Rev. A* **42**, 6052–6059.

Percus, J. K. & Yevick, G. J. [1958] "Analysis of classical statistical mechanics by means of collective coordinates," *Phys. Rev.* **110**, 1–13.

Rabinovich, V. A., Vasserman, A. A., Nedostup, V. I. & Veksler, L. S. [1988] *Thermophysical Properties of Neon, Argon, Krypton and Xenon* (Hemisphere, Washington, DC).

Ravikovitch, P. I., Vishnyakov, A. & Neimark, A. V. [2001] "Density functional theories and molecular simulations of adsorption and phase transitions in nanopores," *Phys. Rev. E* **64**, 011602-1–011602-20.

Sartarelli, S. A., Szybisz, L. & Urrutia, I. [2009] "Adsorption of Ne on alkali surfaces studied with a density functional theory," *Phys. Rev. E* **79**, 011603-1–011603-8.

Sikkenk, J. H., Indekeu, J. O., van Leeuwen, J. M. J. & Vossnack, E. O. [1987] "Molecular-dynamics simulation of wetting and drying at solid-fluid interfaces," *Phys. Rev. Lett.* **59**, 98–101.

Szybisz, L. & Sartarelli, S. A. [2008] "Density profiles of Ar adsorbed in slits of CO_2: Spontaneous symmetry breaking revisited," *J. Chem. Phys.* **128**, 124702-1–124702-8.

Weeks, J. D., Chandler, D. & Andersen, H. C. [1971] "Role of repulsive forces in determining the equilibrium structure of simple fluids," *J. Chem. Phys.* **54**, 5237–5247.